Research Article Open Access

Clove bud extract inhibits glycation of bovine serum albumin: Insights from *in vitro* and molecular dynamics simulation analysis

Saleh A Almatroodi

Department of Medical Laboratories, College of Applied Medical Sciences, Qassim University, Buraydah 51452, Saudi Arabia

*__Correspondence:__ Dr. Saleh A. Almatroodi, PhD, Associate Professor**,** Department of Medical Laboratories, College of Applied Medical Sciences, Qassim University, P.O. Box 6666, Buraydah 51452, Saudi Arabia

Submission Date: September 30th, 2025; **Acceptance Date:** November 7th, 2025; **Publication Date:** November 10th, 2025

Please cite this article as: Almatroodi S. A. Clove bud extract inhibits glycation of bovine serum albumin: Insights from *in vitro* and molecular dynamics simulation analysis. *Functional Foods in Health and Disease*. 2025; 15(11): 818 – 840. DOI: https://doi.org/10.31989/ffhd.v15i11.1762

ABSTRACT

Background: Glycation is a non-enzymatic reaction between amino groups within proteins and reducing sugars, leading to advanced glycation end products (AGEs). AGEs can induce protein cross-linking and accumulate in various tissues. Their buildup contributes to complications associated with chronic disease. Although antiglycation agents like aminoguanidine are well documented, there is a significant need for more effective AGE inhibitors to address various pathogeneses and complications. *Syzygium aromaticum*, commonly known as clove, has several medicinal properties, including antimicrobial and antioxidant effects that contribute to reduced oxidative stress. However, its impact on glycation and related biochemical parameters has not been thoroughly investigated.

Objectives: This study aims to evaluate the impact of clove bud extract on BSA glycation and elucidate its mechanism of action through molecular simulations.

Methods: The antiglycation effects of clove bud extract were evaluated by quantifying glycation-induced changes in BSA structure and aggregation following glucose-mediated glycation and subsequent treatment with varying extract concentrations. UV spectroscopy and fluorescence-based assays (Congo red and Thioflavin T) were used to assess these changes. At the same time, molecular docking and dynamics simulations explored the underlying molecular interactions between clove bud components and BSA.

Results: The results demonstrated that clove bud extract at a 600 µg/ml concentration significantly decreased the browning intensity by 54.38%. When combined with glycated BSA, the extract reduced the aggregation index and mitigated glycation-induced alterations in BSA's secondary structure, indicating its potential to inhibit glycation and prevent AGE formation. Increasing the dosage of clove bud extract resulted in a decrease in Thioflavin T-specific fluorescence in the samples. Molecular docking studies revealed several compounds within the clove extract interact with glycation-prone residues on BSA, specifically lysine and arginine. Molecular simulation studies further confirmed that all tested compounds form stable complexes with BSA when simulated under aqueous conditions, which mirror physiological environments.

Novelty of the Study: This study presents novel findings on the inhibitory effects of clove bud extract on the glycation process of bovine serum albumin (BSA), demonstrating its potential as a natural inhibitor of glycation.

Conclusion: These findings underscore the potential of clove bud as a natural inhibitor of glycation and glycation-induced protein aggregation.

Keywords: Clove; glycation; Oxidative stress, aggregation; BSA; molecular docking; molecular dynamics simulation, Pathogenesis.

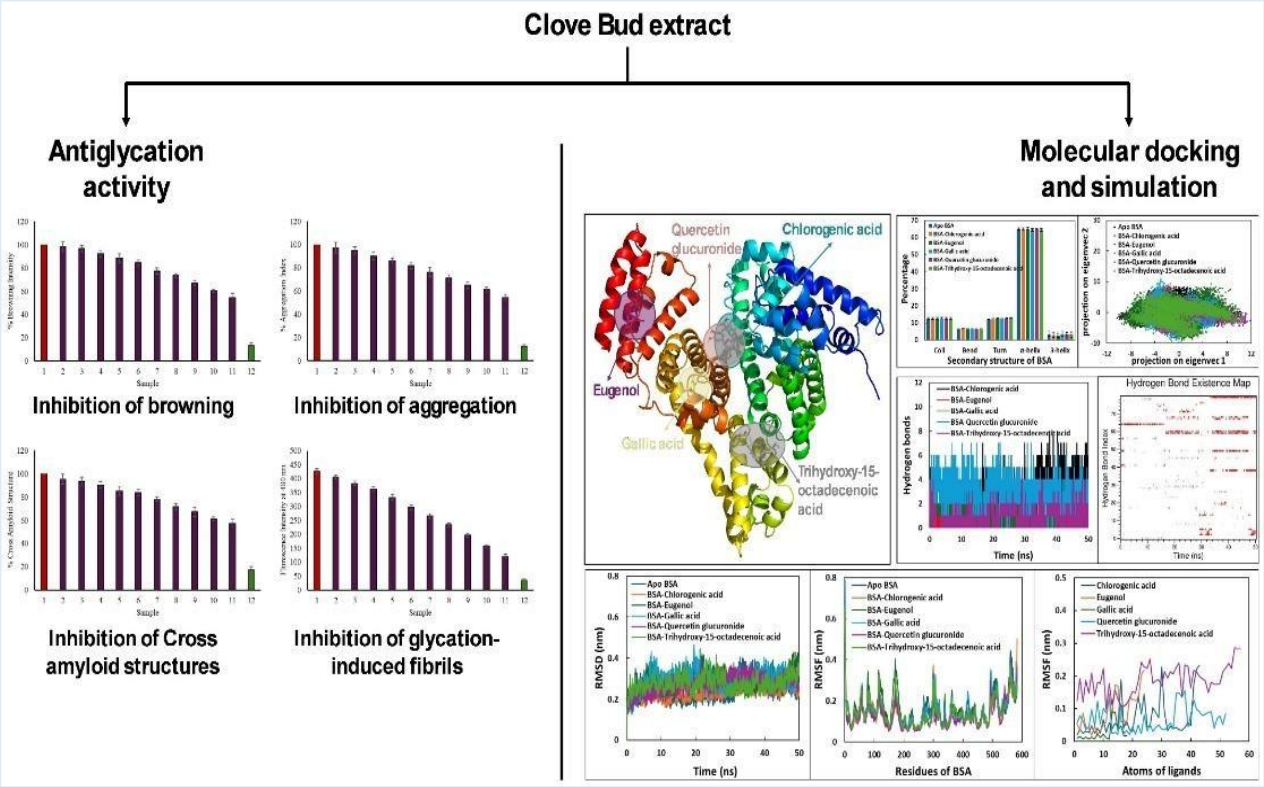

Graphical abstract: Clove bud extract inhibits glycation of bovine serum albumin: Insights from *in vitro* and molecular dynamics simulation analysis

INTRODUCTION

Glycation is a chemical reaction between free amino groups in biological macromolecules (primarily proteins) and reducing sugars or metabolic intermediates produced during glycation. The product of this process is known as advanced glycation end products (AGEs). These AGEs are highly reactive and can form cross-links within proteins; some of them also exhibit specific fluorescence properties [1]. At the onset of hyperglycemia, it accelerates the glycation process, leading to the formation of AGEs that ultimately accumulate as protein aggregates in various tissues [2]. Significantly, glycation-induced structural and functional changes in proteins contribute to diabetes-related complications, including neuropathy, nephropathy, retinopathy, and cardiovascular issues [3, 4]. The accumulation of AGEs damages tissues by generating reactive oxygen species (ROS) and altering the expression of specific genes. The altered expression of genes related to NADPH oxidase and antioxidant enzymes may contribute to diabetic complications and certain age-related disorders [5].

Serum albumin, a major transport protein, is crucial for the transport of numerous exogenous and endogenous compounds. Given its abundance among plasma proteins, it is particularly susceptible to glycation—a process where sugars react with amino groups. This glycation reaction can lead to protein fibrillation, which results in the formation of amyloid-like aggregates. Unfortunately, these aggregates can cause neuronal toxicity [6]. The severity of these pathological complications induced by glycation warrants the need to identify or develop effective glycation inhibitors. While aminoguanidine is a well-known antiglycation agent, its severe adverse effects led to its withdrawal during the third phase of clinical trials [7]. Consequently, there remains a critical need to develop inhibitors of AGEs (advanced glycation end products) that can mitigate the complications associated with diabetes.

Numerous plant extracts and phytocompounds have been documented to inhibit glycation [8]. In a study examining natural extracts, *C. cochinchinense* demonstrated potent inhibition of glycation, achieving over 90% inhibition at 2.5 µg/ml. Similarly, *Cortex magnoliae* officinalis extract showed comparable glycation inhibition, but at a higher concentration of 6.25 µg/ml during in vitro glycation of BSA [9]. *Withania somnifera* ethanolic extract showed promise as an antiglycation agent. Its effect on tail tendon collagen in male Wistar rats was comparable to that of metformin. Researchers attributed this antiglycation effect to the antioxidant properties of the plant's active components. Notably, treatment with *Withania* extract led to a 79% increase in solubility in the pepsin-treated tail tendon, indicating reduced collagen cross-linking [10-11]. Other plant extracts, including *Aralia taibaiensis*, *Asparrausi officinalis*, *Acanthopanax senticosus*, *Ophiopogon japonicus*, *Panax notoginseng*, *Poria cocos*, and *Polygala tenuifolia*, also exhibited significant antiglycation effects in glucose-mediated glycation of BSA at a concentration of 1 mg/ml [11]. Recent studies have reported that natural products, including polyphenols derived from the leaves of Apium graveolens (celery) and broccoli seed extract, exhibit anti-glycation properties [12-13].

Syzygium aromaticum (clove), a member of the Myrtaceae family, is cultivated in tropical regions such as Indonesia, Sri Lanka, southern India, Brazil, China, and Malaysia [14]. This plant is renowned for its diverse medicinal properties, which act through various mechanisms of action [15]. Clove flower buds have been shown to inhibit the glycation of BSA, as indicated by reduced BSA migration in PAGE analysis on day 30 when treated with 10 µg/ml clove extract [16-17]. Clove bud extract is rich in phenolic compounds, including eugenol, eugenol acetate, and gallic acid. These compounds contribute to its potent antioxidant properties. These compounds neutralize free radicals, thereby mitigating oxidative stress and reducing the risk of chronic diseases,

including cardiovascular disorders, cancer, and neurodegenerative conditions [18]. However, recent advancements in analytical techniques, such as HPLC and GC-MS, have enabled precise quantification of its bioactive components. Additionally, in vitro and in vivo studies using cellular and animal models have demonstrated its protective effects against oxidative stress. Novel assays such as ORAC, DPPH, and ABTS are used to measure its antioxidant capacity, while nanotechnology applications, including nanoencapsulation, enhance its stability and bioavailability [19]. Despite these findings, a comprehensive investigation into the effects of clove bud extract on glycation and its underlying mechanisms remains unexplored. This study aims to evaluate the impact of clove bud extract on BSA glycation and elucidate its mechanism of action through molecular simulations.

MATERIAL AND METHODS

Materials: BSA lyophilized powder, purity ≥96%, Glucose ≥99.5% purity, Thioflavin T, and Congo Red having a purity of ≥97.0%, sodium azide having purity of ≥99.5%. Dimethyl sulfoxide (DMSO), Hydrochloric Acid (36%), Ethanol (≥99.5% pure), and Methanol (≥99.9% pure) were sourced from Merck, Darmstadt, Germany. All other solvents and reagents used were of HPLC grade, ensuring high purity and suitability for analytical applications.

Gathering Clove Buds and Extract Preparation: Clove buds, air-dried and acquired from an herbal supplier in Buraydah, Qassim, were used for extraction. The methanolic extraction process followed a standardized approach similar to that in prior tests [20]. Initially, the cloves were washed with distilled water and dried in a shaded area. Once dehydrated, they were finely ground using a digital grinder. For extraction, 100 grams of powdered cloves were macerated in 1000 mL of 97% methanol at 37°C with 24 hours of continuous stirring using a magnetic stirrer. After extraction, the mixture was filtered using Whatman filter paper under ambient conditions, with a temperature below 40°C. The resulting methanolic extract was stored at 4°C. The yield percentage of the extract was calculated using the formula:

$$Yield(\%) = \frac{Weight of sample extract}{Initial weight of sample} \times 100$$

Clove bud extract is a complex mixture of compounds, dominated by eugenol, which constitutes 72-90% of the extract. Other significant components include β-caryophyllene (5-12%), α-humulene (0.55-1.2%), and eugenyl acetate (1-6%), gallic acid (1.5-2.5%), quercetin glucuronide (0.5-1%), and chlorogenic acid (0.1-0.5%). The extract's qualitative composition features phenylpropanoids like eugenol and its derivatives, sesquiterpenes including β-caryophyllene and α-humulene, monoterpenes such as limonene and β-pinene, and other compounds like vanillin and methyl salicylate. The composition can vary with factors like geographical origin, extraction method, and storage. These variables influence its aroma, flavor, and biological activities [19-22].

Incubation of clove bud extract with in vitro glycation system: The in vitro glycation assay of bovine serum albumin (BSA) adhered to the standard protocol [23] with recent adaptation [24]. Sterile experimental conditions were ensured through autoclaved, closed-capped glass vials. BSA at 0.010 g/mL and glucose at 0.50 M were mixed in a 100 mM phosphate buffer with pH 7.4. The reaction mixture was supplemented with varying concentrations of clove bud extract (ranging from 50 to 600 µg/ml). The prepared vials were then stored at 37°C for 15 days in a dark environment to facilitate glycation. Following incubation, the glycated BSA samples were diafiltrated overnight at 37°C against 50 mM phosphate buffer (pH 7.4) to remove excess glucose. The BSA quantification was performed based on its specific molar extinction coefficient. After dialysis, the samples were

stored at -20°C pending further analysis. This procedure was meticulously replicated thrice to ensure the reliability of the data obtained.

Effect of clove bud extract on browning in glycated samples: The extent of browning in glycated specimens is a robust indicator of glycation levels[24]. After post-dilution with distilled water, browning intensity was quantified spectrophotometrically by measuring absorbance at 420 nm in a 1 cm path length spectrophotometric cell23. These measurements were conducted in triplicate to ensure data accuracy. The relative browning intensity, expressed as a percentage, was calculated using the pertinent equation [24].

$$Percentage\ browning\ intensity\ inhibitio = \frac{(Nc - Ns)}{Nc} \times 100$$

The absorbance of the test solution having BSA and glucose system (lacking extract) or the control is Nc; the absorbance of the test solution with BSA and glucose system (with extract or the treated solution) is Ns.

Effect of clove bud extract on protein aggregation index: The aggregation index is an indirect metric for quantifying sample protein aggregation levels. As delineated earlier[25], this index is recognized as an indirect indicator of protein aggregation. The percentage of protein aggregation index for various glycated samples was calculated by measuring absorbance at 280 nm and 340 nm using spectrophotometry.

$$Proteina\ ggregation\ index(\%) = \frac{N_{340}}{(N_{280} - N_{340})} \times 100$$

N_{340} is the absorbance of the test sample at 340 nm, and N_{280} is the absorbance of the same sample at 280 nm.

Determination of fibrillar state by Congo red assay: Congo red has an affinity for amyloid structures through the electrostatic interactions between its negatively charged sulfonic acid groups and the positively charged amino acid residues present on the surfaces of protein molecules, as elucidated earlier [26] and followed as earlier [27]. Glycation can stimulate this process. The preparation of Congo Red was conducted according to the protocols specified in prior research[24]. The assay measured the absorbance of AGEs-modified BSA alone, AGEs-BSA in the presence of clove bud extract, native BSA, and a background control containing Congo red. For the assay, 0.10 mL of Congo red was mixed with 0.50 mL of either AGEs-BSA or native BSA, and the mixture was incubated at 37°C for 10 minutes. Following incubation, the absorbance at 530 nm was recorded for each sample to assess the presence of amyloid fibrils.

$$Amyloid\ formation\ inhibition(\%) = \frac{(Nc - Ns)}{Nc} \times 100$$

The absorbance of the test solution having BSA and glucose system (lacking extract) or the control is Nc; the absorbance of the test solution with BSA and glucose system (with extract or the treated solution) is Ns.

Biophysical investigations: Protein aggregation can be assessed using various methodologies in both in vivo and in vitro settings. Techniques such as transmission electron microscopy/atomic force microscopy (TEM/AFM), molecular probes, and spectroscopic methods, such as circular dichroism (CD) and Fourier-transform infrared spectroscopy (FTIR), have been used to quantify aggregation in vitro. In contrast, indicators such as changes in the enzymatic activity of a folding reporter or fluorescence variations of the target protein indicate alterations in aggregations. Additionally, fluorescence microscopy facilitates the direct observation of target protein aggregation in living cells without perturbation. In this context, a suite of biophysical analyses was employed, including absorption spectroscopy, thioflavin T emission spectroscopy for amyloid identification, and fluorescence assays targeting AGEs to evaluate the efficacy of clove bud extract in mitigating protein aggregation. A standard solution of BSA was prepared at a concentration of 1000 µg/ml in a

0.020 M sodium phosphate buffer at pH 7.4. BSA at a 0.2 mg/ml concentration was subjected to non-enzymatic glycation with 0.5 M glucose within the same buffer at an ambient of 37°C for 15 days to induce glycation. A control sample comprising solely BSA in an identical phosphate buffer was a reference. To preclude bacterial contamination, sodium azide was introduced at a concentration of 3 mM. Following incubation, the solutions underwent dialysis against a 0.1 M sodium phosphate buffer at pH 7.4 and a temperature of 4°C. To assess the preventive capability of clove bud extract against glycation product formation and AGE accumulation, BSA (0.2 mg/ml) was reacted with 0.5 M glucose in the presence of the extract at concentrations ranging from 50 to 600 µg/ml in 0.020 M sodium phosphate buffer at pH 7.4. The propensity for AGE formation and resistance to glycation was analyzed using various biophysical techniques.

UV Absorption: Ultraviolet absorption spectroscopy was performed with the utmost precision using a PerkinElmer Lambda 25 dual-beam spectrophotometer. The spectrophotometer meticulously scanned the spectral profiles of assorted samples and distinguished them by their glycated and non-glycated states across the wavelength range of 240 to 500 nm. The absorbance intensities corresponding to each sample were quantitatively assessed at the specific wavelength of 280 nm, ensuring the accuracy of our results [28].

AGE-specific fluorescence study: The inhibitory effect on fluorescent AGE formation was thoroughly assessed using a Shimadzu RF-5301PC spectrofluorometer. Fluorescence was excited at 350 nm, and emission spectra were recorded from 400 to 480 nm. The apparatus was set with a slit width of 3 nm for both the excitation and emission paths, ensuring the validity of our findings [28]. To correct the inner filter effect in fluorescence spectroscopy, the following formula was used in all the data calculations in this study [29]:

$$F_{corrected} = F_{measured} \times 10^{(A_{ex}/2 + A_{em}/2)}$$

Where, $F_{corrected}$ is the corrected fluorescence intensity, $F_{measured}$ is the measured fluorescence intensity, A_{ex} = Absorbance of the sample at the excitation wavelength, and A_{em} = Absorbance of the sample at the emission wavelength.

Thioflavin T-specific fluorescence study: The comprehensive thioflavin T-specific fluorescence study investigated the ability of clove bud extract to suppress fibril formation induced by glycation. Each specimen was treated with a 6 M solution of Thioflavin T, and subsequent fluorescence measurements were taken, spanning an emission wavelength range of 450-600 nm. In contrast, the excitation wavelength was fixed at 440 nm. For both excitation and emission pathways, the spectrophotometer was configured with a slit width of 10 nm, ensuring the thoroughness of our research [28].

Molecular Docking: Researchers have discovered that certain compounds, including gallic acid, chlorogenic acid, quercetin glucuronide, eugenol, and trihydroxy-15-octadecenoic acid, are active constituents of clove buds [30-31]. Molecular docking of these compounds with BSA was performed to examine binding affinity and binding sites. To perform these calculations, we utilized AutoDock Vina, a software known for its accuracy and computational efficiency compared to the standard AutoDock [32-33]. The three-dimensional crystal structure of BSA was obtained from the RCSB Protein Data Bank (PDB: 4F5S). We removed all water molecules from the receptor to prevent interference during docking calculations. Additionally, we merged non-polar hydrogens and assigned Kollman charges, saving the modified structure in PDBQT format using MGL Tools-1.5.6[34]. For the docking simulations, we defined a grid with dimensions of 94 Å × 62 Å × 76 Å, with a 1 Å spacing, effectively covering the entire BSA molecule. The grid center coordinates were x = 8.806, y = 23.323, z = 102.451. The 3D structures of ligands were taken from

the PubChem database in SDF format. Using Chimera 1.14, we converted it to PDB format and made the ligand flexible by identifying its rotatable bonds. Finally, the ligand structure was saved in PDBQT format. Post-modeling analyses were conducted using Discovery Studio 2024 and PyMOL 3.0.

Molecular dynamics simulations: Furthermore, we investigated the behavior of BSA and the complexes with phytocompounds of clove buds using molecular dynamics (MD) simulations. To perform these simulations, we employed the Amber99SB-ILDN force field in GROMACS 2018 [35-36]. The topology of ligands was prepared using the Amber99sb force field in the Antechamber package of AmberTools19 [37]. Subsequently, we solvated the systems in cuboidal boxes using the TIP3P water model. To maintain charge neutrality, we introduced 16 sodium ions, then added 150 mM NaCl to match physiological salt levels. The energy minimization was performed using the steepest descent method to eliminate weak Van der Waals interactions. After the energy minimization, the system underwent equilibration in two distinct stages. In the first stage, simulations were performed using the NVT ensemble, which maintains a fixed volume while regulating the temperature. The temperature was maintained at 310 K using the V-rescale thermostat, and this phase lasted for 1 nanoseconds[38]. Subsequently, the second stage employed the NPT ensemble, wherein both pressure (1 bar) and temperature (310 K) were maintained. This was achieved using the Parrinello-Rahman barostat, and the system was allowed to equilibrate for an additional 1 nanosecond[39]. The MD simulations were performed over 50 nanoseconds, during which we saved 5,000 frames at 10-ps intervals. Before analysis, we corrected the trajectory for periodic boundary conditions (PBC). Using Gromacs utilities, root mean square deviation (RMSD), radius of gyration (Rg), root mean square fluctuation (RMSF), solvent accessible surface area (SASA), and hydrogen bonds analysis were performed. Additionally, we evaluated the binding energies between ligands and BSA, as well as the contribution of each residue to the overall energy, using MM-PBSA calculations [40].

Software and Statistical Analysis: Data analysis and statistical evaluations were performed using the IBM SPSS Statistics 30.0.0. Given that the study involves comparing multiple treatment groups to a single glycated control, a one-way ANOVA followed by a post hoc test, such as Dunnett's test, was used for the analysis. Error bars represent the Mean ± Standard Deviation (SD).

The following software packages were used for in silico studies.

Discovery Studio 2024: Used for post-modeling analyses of molecular docking results.

PyMOL 3.0: Utilized for visualization and analysis of molecular docking results.

GROMACS 2018.1: Employed for molecular dynamics simulations.

AmberTools19: Used for topology preparation of ligands for molecular dynamics simulations.

AutoDock Vina: This software was used for performing molecular docking simulations.

MGL Tools-1.5.6: Used to prepare the receptor and ligand structures for use with AutoDock Vina.

Chimera 1.14: Used for converting ligand structures from SDF to PDB format and preparing flexible ligands.

RESULTS

Browning intensity investigation

We investigated the impact of clove bud extract on browning reactions, specifically its ability to mitigate early glycated-BSA formation. We measured the absorbance at 420 nm to determine the variation in intensity between glycated-BSA samples treated with clove extract and untreated glycated-BSA samples. Intense brown pigments become apparent during the initial phase of the three-step chemical process, leading to the formation of AGEs. Our results demonstrate that the addition of clove bud extract significantly reduces the browning intensity in glycated-BSA samples. At a 600 concentration of µg/ml, the clove bud extract suppressed browning intensity by 54.38% at the end of the study period. Conversely, maximal browning, equivalent to 100% browning, was observed in the glycated BSA samples that were incubated without the extract (Fig. 1). Glycoproteins and advanced glycation end products (AGEs) represent distinct stages in nonenzymatic browning. Initially, glycoproteins emerge due to covalent crosslinking between proteins and reducing sugars. Subsequently, AGEs are the ultimate products of this browning reaction [41].

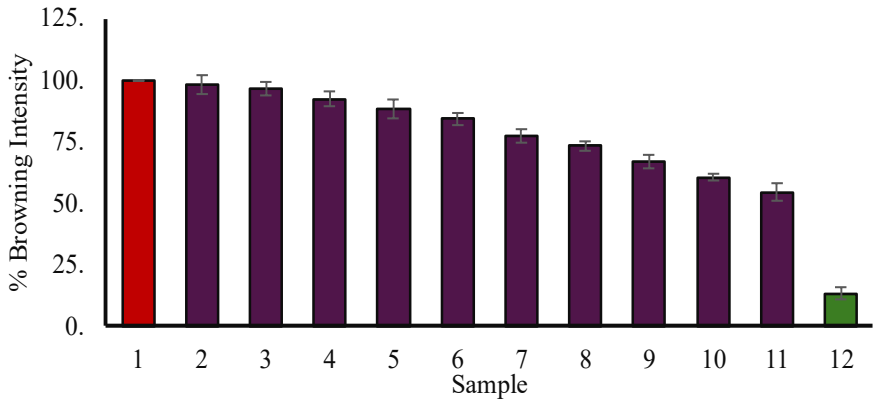

Fig 1. Decrease in browning intensity when clove bud extract is present. BSA was kept in the presence of glucose for 15 days. In sample 1 (red column), it is thought to have glycated to 100% of its original state (browning). Sample 2-11 (magenta columns) contained 50, 75, 100, 150, 200, 250, 300, 400, 500, and 600 µg/ml of clove buds, and browning or glycation is displayed to be lower as the extract concentration increases. BSA was kept for the same period (15 days) in sample 12 (green column) without extract or glucose. The p-value was found to be lower than 0.05 (n=3, $p < 0.05$).

Effect of methanol extract on protein aggregation Index; Protein aggregation resulting from glycation occurs when the carbonyl group of glucose interacts with proteins. This glycation process leads to structural and functional changes in proteins, and it can occur at various sites, including the side chains and N-terminal groups of polypeptides. Additionally, glycation promotes the formation of protein aggregates by triggering the clustering of carbonyl groups bound to proteins. The formation and implications of protein aggregates in various diseases have been extensively studied. In this study, we investigated the impact of clove bud extract on the formation of amyloid cross-structures when incubated with sugars and proteins. By analyzing the aggregation index, we found that clove bud extract reduced the formation of amyloid cross-structures. The BSA-glycation system exhibited the highest level of aggregation. However, the clove bud extract significantly attenuated glycation-induced aggregation in glycated BSA. Figure 2 showed that samples of glycated BSA incubated with clove bud extract demonstrated a lower aggregation index than those without extract. Maillard reactions have a significant impact on the functional properties of proteins. Notably, these reactions can lead to protein unfolding and aggregation [42].

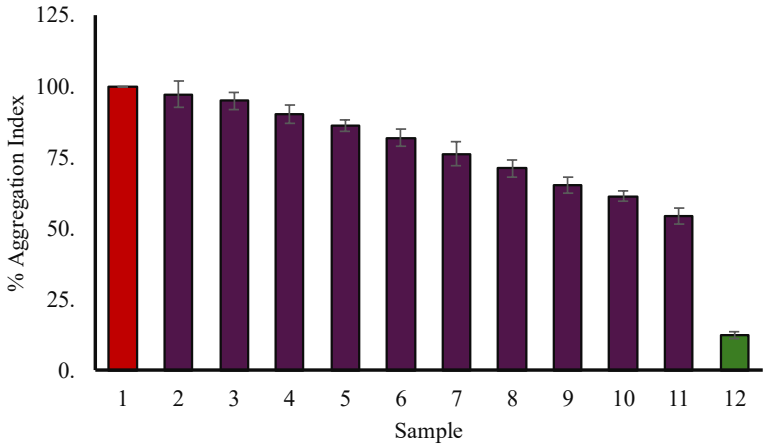

Fig 2. Reduction in aggregation index when clove bud methanol extract is present. Sample 1 is BSA kept with glucose for 15 days and displayed the highest aggregation index and, consequently, the maximum glycation. Clove bud (magenta column) methanol extract was present in samples 2-11 at concentrations ranging from 50, 75, 100, 150, 200, 250, 300, 400, 500, and 600 µg/ml. The aggregate index is demonstrated to decrease as the clove bud extract concentration increases (magenta column). Sample 12 (green column) contained BSA that was kept alone and displayed a minimum aggregation index. The p-value significance was noticed to be a value lower than 0.05 (n=3, $p < 0.05$).

Congo red (CR) assay: Glucose has been found to cause changes in the secondary structure of BSA, making the glycation-prone sites more accessible to the solvent on the surface area. The Congo Red (CR) method, which involves measuring specific absorption at 540 nm after binding, is a well-established technique for assessing the presence of cross-structures in glycated proteins [24,43]. In our experiments, CR-glucose samples exhibited an increase in intensity at 540 nm, indicating the presence of amyloid-specific structures. However, with the addition of clove extract, the glycation-induced alteration of the native BSA's canonical secondary structure was reduced. As observed in Fig. 3, the glycated samples treated with clove bud extract demonstrated a dose-dependent reduction in BSA fibrillation.

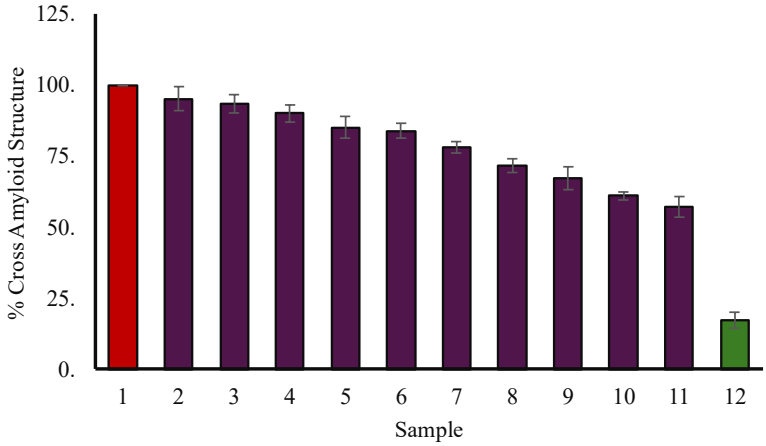

Fig 3. Cross amyloid structures are reduced when clove bud extract is present (magenta column). Sample 1 is BSA that has been placed with glucose over fifteen days; it is believed to have 100% amyloid fibrils in the current study as it has been determined to have the maximum structural modifications. The cross-amyloid structures appear reduced with increasing clove bud extract concentration in Sample 2-11, which contained 50, 75, 100, 150, 200, 250, 300, 400, 500, and 600 µg/ml of extract (magenta column). Sample 12 (green column), which contained BSA only (incubated alone), displayed the fewest cross-amyloid structures. The p-value significance was noticed to be a value lower than 0.05 (n=3, $p < 0.05$).

UV-Absorption studies: Proteins undergo conformational changes because of non-enzymatic glycation. Previous studies have observed a significant absorption peak at 280 nm in BSA samples incubated with glucose alone, indicating notable hyperchromicity compared to native BSA incubated without glucose. This hyperchromicity at 280 nm in non-enzymatically glycosylated samples may be attributed to alterations in aromatic residues and the microenvironment of amino acid residues [28]. Interestingly, our findings demonstrate that as the concentration of clove bud extract increased, the hyperchromicity observed in the different samples significantly decreased, as shown in **Fig. 4**. These results suggest that the extract may play a role in mitigating the conformational changes induced by non-enzymatic glycation in proteins.

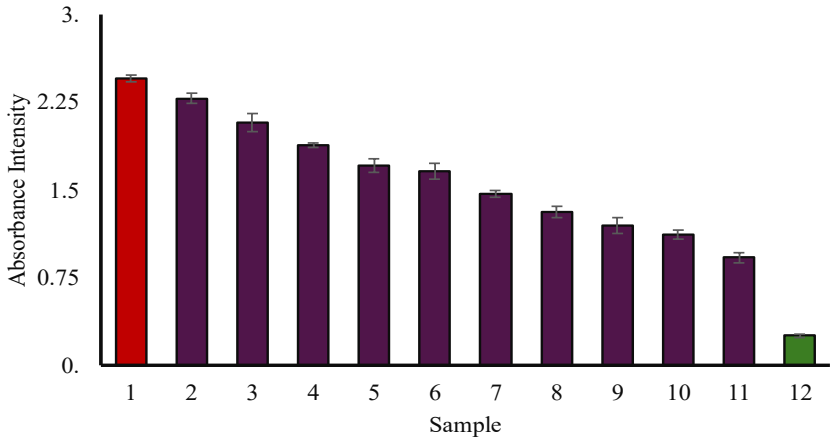

Fig 4. Absorbance declines when clove bud extract is present. Sample 1 is BSA incubated with glucose for 15 days, and it appears to exhibit the most significant structural changes. 50, 75, 100, 150, 200, 250, 300, 400, 500, and 600 µg/ml of extract were present in samples 2-11 (magenta column). Sample 12 (green column) contained BSA that had been incubated without any extract or glucose. The p-value significance was noticed to be a value lower than 0.05 (n=3, $p < 0.05$).

Effects of extract on fluorescent AGE formation: As reported in previous studies, BSA samples incubated with glucose exhibited the highest fluorescence intensity at 450 nm [28,44]. To evaluate the anti-glycation activity of clove bud extract, a methanol extract of clove buds was tested on the fluorescent AGE formation in BSA samples incubated with glucose. BSA is a major plasma protein that can undergo glycation and form AGEs. The fluorescence intensity of AGEs at 450 nm reflects the degree of glycation. As observed in Fig. 5, BSA samples incubated with glucose alone showed the highest fluorescence intensity, indicating the highest level of glycation. However, when clove bud extract was added to the BSA-glucose mixture, the fluorescence intensity decreased in a dose-dependent manner, reaching the lowest level at 600 µg/ml of clove bud extract. This indicates that clove bud extract can inhibit the glycation of BSA and prevent the formation of AGEs. Clove bud extract may contain phenolic compounds that can scavenge reactive carbonyl species and block the glycation reaction. These findings highlight the potential of clove bud extract in the field of biochemistry and pharmacology, offering a promising avenue for future research and applications.

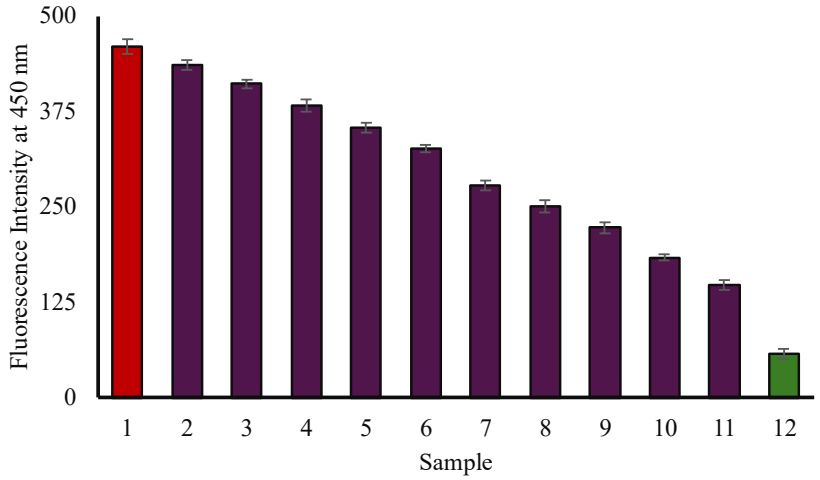

Fig 5. Fluorescence intensity (at 450 nm) declines when clove bud extract is present. Sample 1 is BSA incubated with glucose for 15 days, and it appears to exhibit the most significant structural changes. 50, 75, 100, 200, 250, 300, 400, 500, and 600 µg/ml of extract were present in samples 2-11 (magenta column). Sample 12 (green column) contained BSA that had been incubated without any extract or glucose. The p-value significance was noticed to be a value lower than 0.05 (n=3, $p < 0.05$).

Effect of clove bud extract on the formation of glycation-induced fibrils: Thioflavin T (ThT) is commonly utilized to investigate the formation of amyloid fibrils in glycated samples [28]. In its free state, ThT exhibits weak fluorescence. However, upon interaction with fibrils formed in glycated proteins, ThT's fluorescence intensity increases significantly. In the case of BSA glycated by glucose, ThT fluorescence at 480 nm increases, indicating the formation of fibrils due to BSA glycation. Our study found that as the dosage of clove bud extract in the incubated samples increased, there was a gradual reduction in ThT-specific fluorescence at 480 nm in the presence of the extract (Fig. 6). The most robust ThT-specific fluorescence at 480 nm was observed in BSA treated with glucose alone. These findings suggest that clove bud extract protects against the synthesis of AGEs induced by glycation. Still, they also reassure us about the increasing level of protection displayed by the extract, alongside the concentration of clove bud extract used.

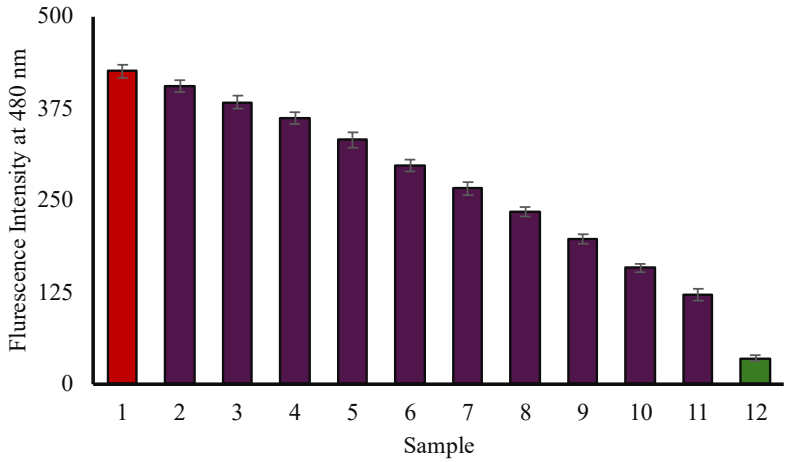

Fig 6. Fluorescence intensity (at 480 nm) declines when clove bud extract is present. Sample 1 is BSA incubated with glucose for 15 days, and it appears to exhibit the most significant structural changes. 50, 75, 100, 150, 200, 250, 300, 400, 500, and 600 µg/ml of extract were present in samples 2-11 (magenta column). Sample 12 (green column) contained BSA that had been incubated without any extract or glucose. The p-value significance was noticed to be a value lower than 0.05 (n=3, $p < 0.05$).

Molecular Docking: We conducted molecular docking studies involving the ligands and BSA to examine the interaction. Notably, these ligands exhibited a range of affinity toward BSA. Quercetin glucuronide showed the highest affinity towards BSA out of all docked compounds. The binding affinity of chlorogenic acid, eugenol, gallic acid, quercetin glucuronide, trihydroxy-15-octadecenoic acid with BSA was found to be -7.7, -6.6, -6.2, -9.3, and -7.1 kcal/mol. The overlap of all ligands in BSA is shown in Fig. 7A. Arg435, Ile455, Ser428, Ala193, Ser192, Glu424, Thr190, Leu189, His145, Arg144, Asp108, Arg458, and Pro110 of BSA interacted with chlorogenic acid via different non-covalent forces (Fig. 7B). Similarly, eugenol interacted with Phe550, Phe508, Phe506, Gln579, Ley574, Ala527, Leu528, Val575, His534, Leu531, Phe501, and Thr578 and its interaction diagram is shown in Fig 7C. For the complexation of gallic acid with BSA, Cys391, Thr448, Cys436, Cys437, Gly433, Leu429, Phe402, Val432, Leu452, Tyr410, Arg409, Leu406, Asn390, and Leu386 were involved (Fig 7D). Moreover, molecular docking revealed that His145, Asp108, Arg458, Leu189, Ala193, Glu424, Ser428, Arg427, Lys431, Leu454, Ile455, Tyr451, Thr190, Arg435, Glu186, Arg196, Ser192, and Arg144 of BSA were interacting with quercetin glucuronide as presented in Fig. 7E. The binding of trihydroxy-15-octadecenoic acid with BSA involved Val215, Gly327, Leu330, Leu326, Glu353, Leu346, Ala349, Arg208, Val481, Lys350, Leu480, Ser479, Phe205, Ala209, Ala212, Asp323, and Lys211 residues Fig 7F. In protein glycation, lysine residues are known to be the most susceptible to glycation. Numerous proteins, including hemoglobin, lysozyme, and albumin, have highlighted lysine as a hotspot for this chemical modification. Notably, arginine, histidine, and cysteine have also been documented to undergo glycation[45]. Interestingly, many tested compounds of clove bud have been found to interact directly with BSA's arginine and lysine residues. Once the ligand masks these glycation-prone residues, the chances of glucose and glycation attachment are reduced.

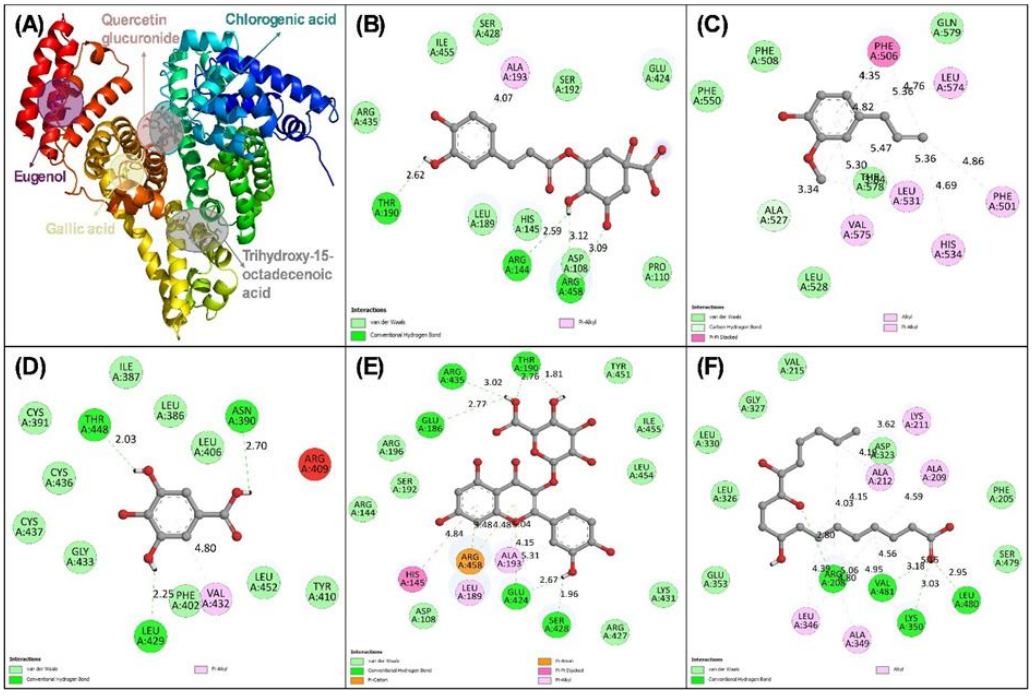

Fig 7. Molecular docking analysis of BSA–ligand complexes (A) Overlap of all docked poses of ligands in BSA. (B) Two-dimensional representation of docked HSA-chlorogenic acid complex. (C) Two-dimensional representation of docked HSA-eugenol complex. (D) Two-dimensional representation of docked HSA-gallic acid complex. (E) Two-dimensional representation of docked HSA-quercetin glucuronide complex. (F) Two-dimensional representation of docked HSA-trihydroxy-15-octadecenoic-acid complex.

Molecular dynamics simulations: To explore the stability and behavior of the BSA and the complexes in an aqueous environment, we conducted molecular dynamics (MD) simulations. We chose the docked conformation with the lowest binding energy for these simulations. We performed root-mean-square deviation (RMSD) analysis, which tracks how each system's backbone deviates from its initial structure over time. Notably, the RMSD of apo BSA showed some deviations but eventually stabilized in the early simulation stage (as depicted in Fig. 8A). Similarly, all complexes exhibited similar RMSD yet consistently remained below 0.4 nm throughout the simulation. This data suggests that all systems achieved stability in the early simulation stage [46]. Calculating average RMSD values, we found them to be 0.247 nm for apo BSA, 0.226 nm for BSA-chlorogenic acid complex, 0.290 nm for BSA-eugenol complex, 0.293 nm for BSA-gallic acid complex, 0.272 nm for BSA-quercetin glucuronide complex, and 0.276 nm for BSA-trihydroxy-15-octadecenoic acid complex. We also calculated the root mean square fluctuations (RMSF) of Cα atoms of all residues of BSA in the absence and presence of ligands (Fig. 8B). Even in the presence of ligands, most BSA residues exhibited an RMSF of 0.20 nm, indicating the stability of ligands when in a complex with BSA [46]. Furthermore, our RMSF analysis of ligands showed some movement at the binding site in BSA (Fig. 8C), potentially influencing interactions with neighboring residues [46].

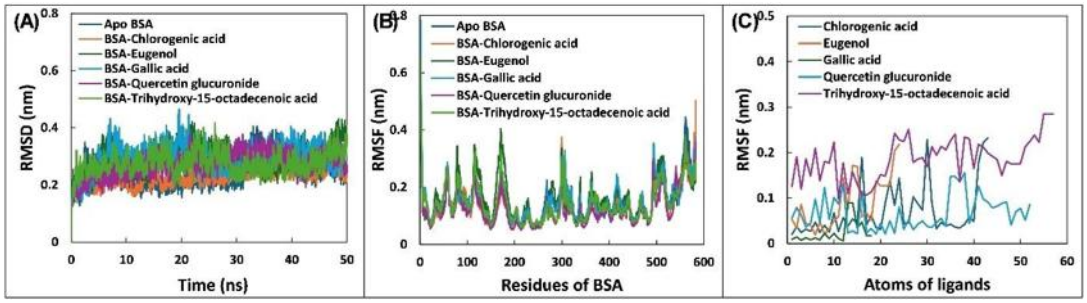

Fig 8. Molecular dynamics analysis of BSA–ligand complexes (A) Root mean square deviation (RMSD) of apo BSA, BSA-chlorogenic acid complex, BSA-eugenol complex, BSA-gallic acid complex, BSA-quercetin glucuronide complex, and BSA-trihydroxy-15-octadecenoic acid complex during 50 ns MD simulation. (B) Average root mean square fluctuation (RMSF) of residues of BSA without or with chlorogenic acid, eugenol, gallic acid, quercetin glucuronide, or trihydroxy-15-octadecenoic acid. (C) Average RMSF of atoms of chlorogenic acid, eugenol, gallic acid, quercetin glucuronide, or trihydroxy-15-octadecenoic acid.

To explore how , we investigated key parameters, including the radius of gyration (R_g), solvent-accessible surface area (SASA), potential energy, and total energy[47]. Fig. 9A depicts the R_g values for BSA in the presence and absence of ligands. Notably, R_g remained consistently around 2.7 nm throughout the simulation. Similar trends in R_g for all complexes were observed throughout the simulation. For example, the average R^g values for apo BSA, BSA-chlorogenic acid complex, BSA-eugenol complex, BSA-gallic acid complex, BSA-quercetin glucuronide complex, and BSA-trihydroxy-15-octadecenoic acid were 2.724, 2.676, 2.743, 2.712, 2.670, and 2.718 nm, respectively. These findings suggest that binding ligands induced minimal changes in BSA's compactness. Fig. 9B shows the SASA profiles of BSA and the complexes over simulation time. The average SASA values were 290.683 nm^2 for apo BSA, 287.775 nm^2 for BSA-chlorogenic acid complex, 292.134 nm^2 for BSA-eugenol complex, 288.573 nm^2 for BSA-gallic acid complex, 286.753 nm^2 for BSA-quercetin glucuronide complex, and 289.255 nm^2 for BSA-trihydroxy-15-octadecenoic acid complex, indicating the overall stability. These negligible variations in R_g and SASA of complexes compared to apo BSA indicate their stable nature under physiological conditions [46], roughly the same as those of apo BSA.

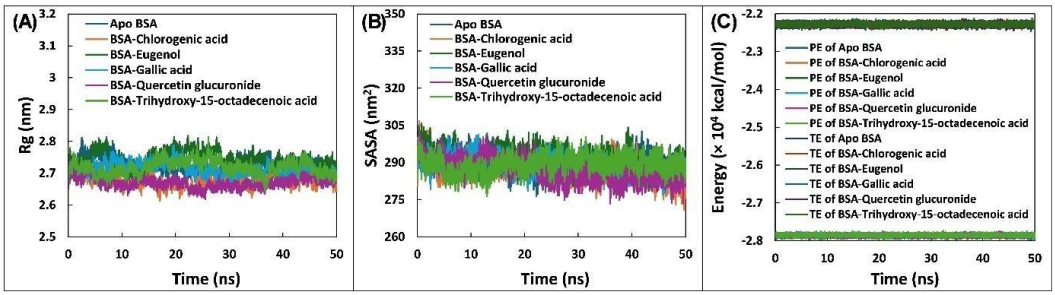

Fig 9. Effect of ligand binding on compactness of BSA (A) Radius of gyration of apo BSA, BSA-chlorogenic acid complex, BSA-eugenol complex, BSA-gallic acid complex, BSA-quercetin glucuronide complex, and BSA-trihydroxy-15-octadecenoic acid complex during 50 ns MD simulation. (B) Solvent accessible surface area (SASA) of apo BSA, BSA-chlorogenic acid complex, BSA-eugenol complex, BSA-gallic acid complex, BSA-quercetin glucuronide complex, and BSA-trihydroxy-15-octadecenoic acid complex during 50 ns MD simulation. (C) Potential energy (PE) and total energy (TE) of apo BSA, BSA-chlorogenic acid complex, BSA-eugenol complex, BSA-gallic acid complex, BSA-quercetin glucuronide complex, and BSA-trihydroxy-15-octadecenoic acid complex during 50 ns MD simulation.

We conducted hydrogen bond analysis to explore the interaction between ligands and BSA (Fig. 10A). The average number of hydrogen bonds formed by chlorogenic acid, eugenol, gallic acid, quercetin glucuronide, and trihydroxy-15-octadecenoic acid with BSA was determined to be 2.350, 0.353, 1.021, 2.940, and 0.858, respectively. It is evident from the data that chlorogenic acid and quercetin glucuronide formed more hydrogen bonds with BSA compared to other ligands. Furthermore, we also examined the hydrogen bond existence profile (Fig. 10B-F), which revealed the hydrogen bond presence throughout the trajectory. In the binding of chlorogenic acid, eugenol, gallic acid, quercetin glucuronide, trihydroxy-15-octadecenoic acid with BSA, Glu424, Leu505, Leu429, Asn457, and Asp323 exhibited the highest occupancy of 29.9%, 29.3%, 56.8%, 79.50%, and 33.5%, respectively.

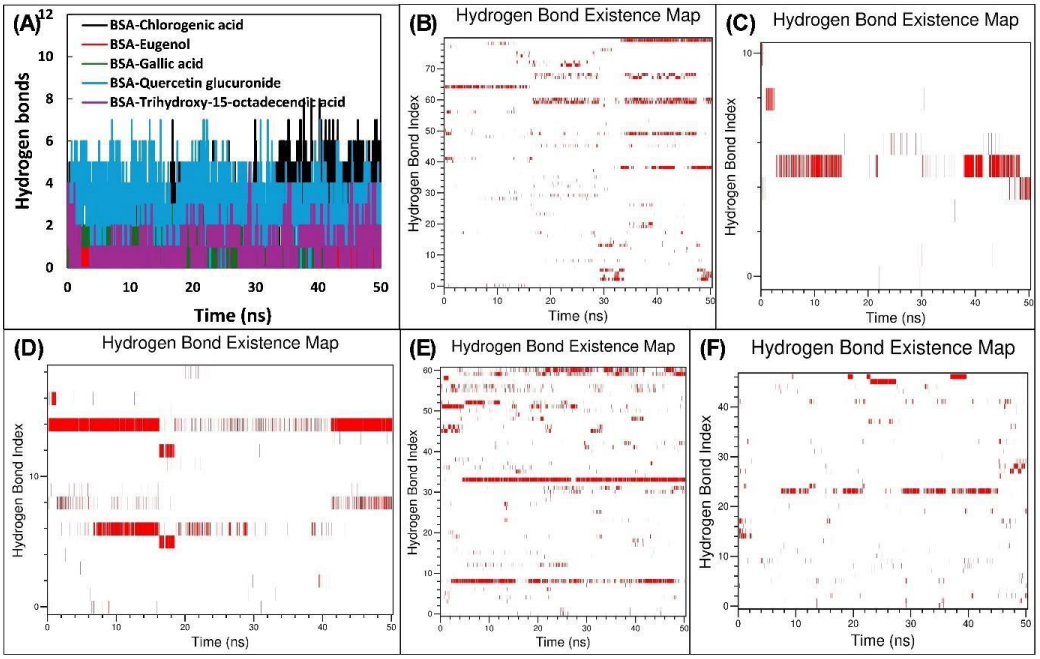

Fig 10. Several hydrogen bonds were formed by Chlorogenic acid, eugenol, gallic acid, quercetin glucuronide, or trihydroxy-15-octadecenoic acid with BSA during 50 ns simulation. (B) Hydrogen bond existence map of BSA-chlorogenic acid complex. (C) Hydrogen bond existence map of BSA-eugenol complex. (D) Hydrogen bond existence map of BSA-gallic acid complex. (E) Hydrogen bond existence map of BSA-quercetin glucuronide complex. (F) Hydrogen bond existence map of BSA-trihydroxy-15-octadecenoic acid complex

We also explored the impact of ligand binding on BSA's secondary structure. Figure 11A presents the average percentages of various secondary structure elements in BSA, both with and without ligands. When BSA was simulated alone, the percentages of coils, bends, turns, α-helices, and 3-helices in apo BSA were 12.746, 6.433, 12.082, 65.207, and 3.484%, respectively. Remarkably, these components showed negligible changes upon ligand binding. For instance, in the BSA-eugenol complex, the average percentages of coils, bends, turns, α-helices, and 3-helices were 12.822, 6.551, 12.798, 65.129, and 2.647%, respectively. This negligible alteration in secondary structure further confirms the stability of all complexes under physiological conditions [48]. Moreover, we employed principal component analysis (PCA), a standard statistical technique for analyzing large-scale motion in biological macromolecules, to examine the flexibility in BSA with and without ligands. PCA reduces the dimensionality of a dataset while retaining essential information, as characterized by its eigenvectors [49]. We compared the flexibility parameters of BSA when it was alone versus when it formed a complex with the ligands. The two-dimensional projections of the eigenvectors for BSA and the complex are shown in Fig. 11B. Interestingly, all complexes occupied a similar conformational space in the two-dimensional projection to that of apo BSA. The data suggest that the flexibility of BSA remained relatively unchanged following the complexation of ligands. To highlight differences, we also visualized free energy landscapes (FELs) for apo BSA and the complexes (Fig. 12). Notably, over a 50 ns MD simulation, apo BSA exhibited three energy minima. Whereas, in trajectories of BSA-chlorogenic acid complex, BSA-eugenol complex, BSA-gallic acid complex, BSA-quercetin glucuronide, and BSA-trihydroxy-15-octadecenoic acid, there were four, four, three, one, and eight energy minima points.

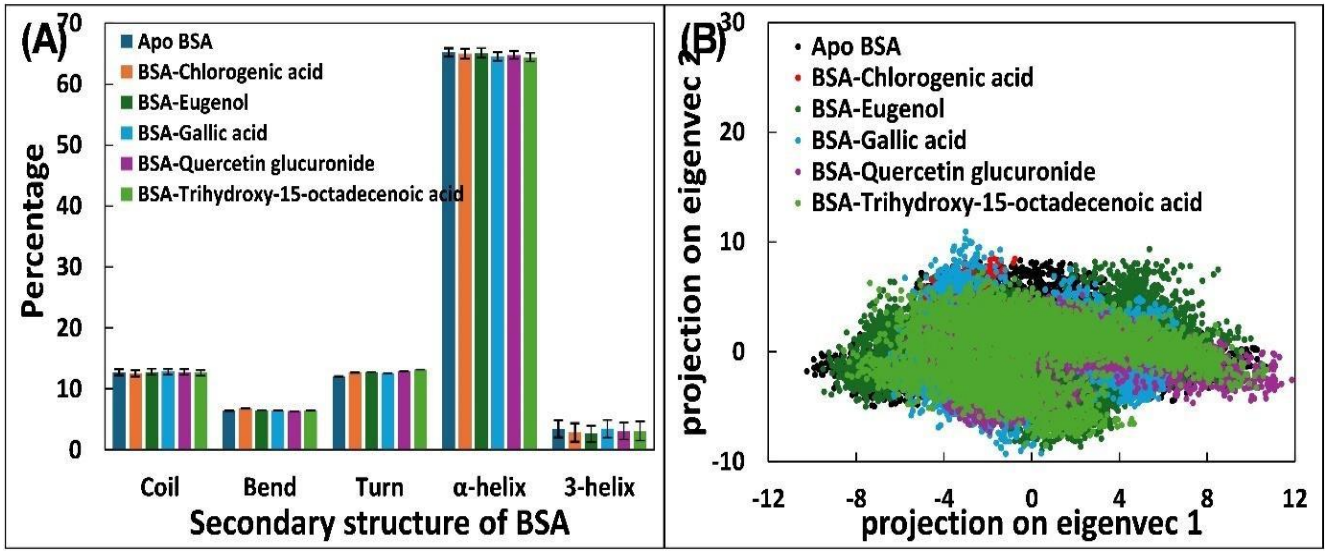

Fig 11. Effect of ligand binding on the secondary structure of BSA (A) Average percentage of secondary structure in BSA without or with chlorogenic acid, eugenol, gallic acid, quercetin glucuronide, or trihydroxy-15-octadecenoic acid. (B) Projection of eigenvectors of apo BSA, BSA-chlorogenic acid complex, BSA-eugenol complex, BSA-gallic acid complex, BSA-quercetin glucuronide complex, and BSA-trihydroxy-15-octadecenoic acid complex.

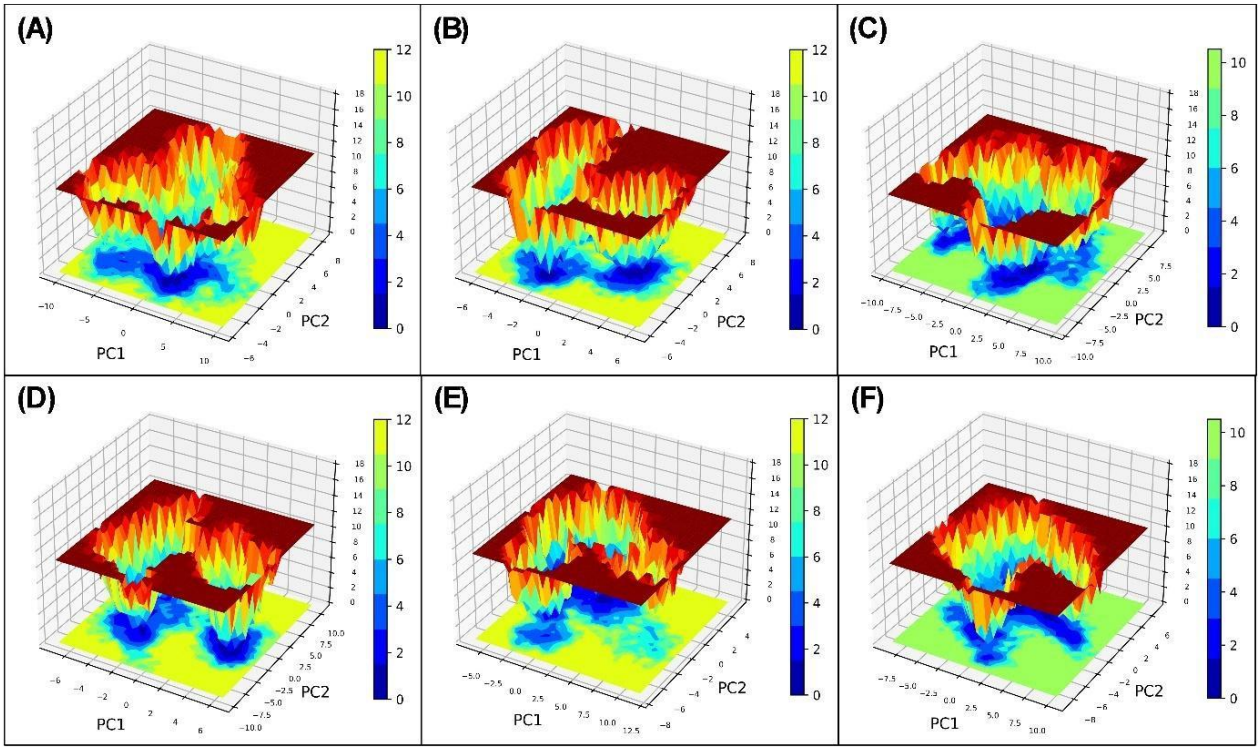

Fig 12. Effect of ligand binding on free energy change in BSA (A) Free energy landscape of apo BSA. (B) Free energy landscape of BSA-chlorogenic acid complex. (C) Free energy landscape of BSA-eugenol complex. (D) Free energy landscape of BSA-gallic acid complex. (E) Free energy landscape of BSA-quercetin glucuronide complex. (F) Free energy landscape of BSA-trihydroxy-15-octadecenoic acid complex.

Finally, we employed MM-PBSA calculations to dissect the various energies involved in complex formation, each exerting a positive or negative influence on the overall binding [50]. In protein-ligand interactions, non-covalent forces play a pivotal role. Among these forces, van der Waals forces, hydrogen bonds, electrostatic forces, and hydrophobic contacts are particularly prominent [51]. The energies associated with this complex formation are summarized in Table 1. In the complexation of chlorogenic acid to BSA, van der Waals energy (-27.076 kcal/mol) and electrostatic energy (-14.605 kcal/mol) were predominant, while a small contribution from SASA (-3.816 kcal/mol) energy. For eugenol and BSA interactions, van der Waal energy (-22.784 kcal/mol) was predominant, with a small contribution from electrostatic energy (-3.371 kcal/mol) and SASA (-2.721 kcal/mol) energy. Similar results were obtained for gallic acid, where van der Waals energy (-24.138 kcal/mol) was a significant contributor, and electrostatic (-5.006 kcal/mol) and SASA (-2.474 kcal/mol) energies made less significant contributions. The remaining two ligands (quercetin glucuronide and trihydroxy-15-octadecenoic acid) also showed a similar pattern in which a significant portion of energy came from van der Waals energy and a lesser portion of energy was contributed by electrostatic and SASA energies. Interestingly, the positive values showed that polar solvation energy (PSA) impeded the overall binding process. Overall, the binding energy for the complexation of chlorogenic acid, eugenol, gallic acid, quercetin glucuronide, and trihydroxy-15-octadecenoic acid with BSA was -9.487, -15.476, -13.629, -24.718, and -26.387 kcal/mol, respectively.

Table 1. MM-PBSA binding energies (kcal/mol) of the compounds of clove bud extract with BSA.

Energy	LIGANDS				
	Chlorogenic acid	Eugenol	Gallic acid	Quercetin glucuronide	Trihydroxy-15-octadecenoic acid
vdW	-27.076±0.465	-22.784±0.284	-24.138±0.163	-52.193±0.426	-43.614±0.381
Elec	-14.605±0.887	-3.371±0.244	-5.006±0.142	-20.621±0.564	-12.033±0.564
PSA	35.963±0.722	13.408±0.309	18.005±0.255	53.040±0.738	34.219±0.592
SASA	-3.816±0.037	-2.721±0.016	-2.474±0.011	-4.989±0.022	-4.982±0.021
BE	-9.487±0.593	-15.476±0.285	-13.629±0.205	-24.718±0.501	-26.387±0.454

vdW is van der Waal energy; Elec is Electrostatic energy; PSA is Polar solvation energy; SASA is SASA energy; and BE is overall Binding energy.

The MM-PBSA analysis also provides insights into the energy contributions from individual amino acids. **Table 2** highlights vital energy-contributing residues within BSA. When examining the interaction between chlorogenic acids, several amino acids stand out as significant contributors: Lys106 (-0.677 kcal/mol), Lys114 (-0.542 kcal/mol), Lys116 (-0.580 kcal/mol), Arg143 (-0.653 kcal/mol), Arg144 (-1.199 kcal/mol), Leu189 (-1.152 kcal/mol), Ala193 (-0.856 kcal/mol), Arg194 (-0.583 kcal/mol), Arg196 (-1.449 kcal/mol), Ile455 (-0.618 kcal/mol), Arg458 (-3.046 kcal/mol), and Lys465 (-0.715 kcal/mol). Similarly, Arg208 (-2.422 kcal/mol), Ala209 (-0.577 kcal/mol), Ala212 (-1.297 kcal/mol), Val215 (-0.897 kcal/mol), Val234 (-0.739 kcal/mol), Lys322 (-0.513 kcal/mol), Ala324 (-0.691 kcal/mol), Leu326 (-1.369 kcal/mol), Gly327 (-0.996 kcal/mol), Leu330 (-0.677 kcal/mol), Tyr331 (-0.481 kcal/mol), and Lys350 (-1.338 kcal/mol) were the primary energy contributing residues in binding of trihydroxy-15-octadecenoic acid with BSA. Interestingly, numerous lysine and arginine residues were among the top energy-contributing residues of BSA. It is well known that lysine and arginine are the primary sites for glycation [52]. The compounds present in clove bud extract may mask these glycation-prone residues, which could be a possible mechanism of glycation inhibition [47].

Table 2. Total energies (kcal/mol) of primary energy contribute residues of BSA to the interaction with compounds of clove bud extract with BSA.

Chlorogenic acid		Eugenol		Gallic acid		Quercetin glucuronide		Trihydroxy-15-octadecenoic acid	
Residues	Total Energy	Residues	Total Energy	Residues	Total Energy	Residues	Total Energy	Residues	Total Energy
Lys106	-0.677±0.018	Phe506	-0.649±0.046	Leu386	-0.442±0.021	Arg185	-0.736±0.048	Arg208	-2.422±0.080
Lys114	-0.542±0.153	Phe508	-0.597±0.034	Ile387	-0.928±0.038	Lys187	-0.639±0.021	Ala209	-0.577±0.035
Lys116	-0.580±0.080	Lys524	-0.108±0.039	Asn390	-0.570±0.064	Leu189	-2.927±0.065	Ala212	-1.297±0.034
Arg143	-0.653±0.026	Ala527	-0.867±0.033	Phe402	-0.641±0.024	Thr190	-0.916±0.062	Val215	-0.897±0.037
Arg144	-1.199±0.092	Leu528	-0.233±0.026	Leu406	-0.730±0.021	Ala193	-1.613±0.038	Val234	-0.739±0.029
Leu189	-1.152±0.084	Glu530	-0.114±0.053	Arg409	-0.950±0.067	Arg194	-1.156±0.033	Lys322	-0.513±0.031
Ala193	-0.856±0.034	Leu531	-0.794±0.047	Lys413	-0.415±0.056	Arg196	-1.488±0.063	Ala324	-0.691±0.041
Arg194	-0.583±0.031	Val546	-0.161±0.032	Leu429	-0.729±0.044	Arg435	-1.306±0.069	Leu326	-1.369±0.033
Arg196	-1.449±0.050	Met547	-0.514±0.041	Val432	-0.753±0.033	Leu454	-1.558±0.054	Gly327	-0.996±0.034
Ile455	-0.618±0.034	Phe550	-1.035±0.063	Gly433	-0.428±0.023	Ile455	-1.551±0.048	Leu330	-0.677±0.023
Arg458	-3.046±0.159	Leu574	-0.461±0.030	Leu452	-1.199±0.023	Arg458	-3.806±0.137	Tyr331	-0.481±0.030
Lys465	-0.715±0.036	Val575	-0.130±0.015	Arg484	-0.579±0.063	Val461	-0.693±0.021	Lys350	-1.338±0.052

DISCUSSION

Antioxidants from various plant and dietary sources play a significant role in disease management through different mechanisms [53-57]. This study explored the antiglycation potential of clove bud extract, focusing on its ability to inhibit glycation-induced alterations in BSA. The results demonstrated a significant reduction in AGE formation, with a 54.38% decrease in browning intensity at 600 µg/ml, highlighting its promise as a natural inhibitor of protein glycation and its associated complications. These findings align with previous studies on plant extracts such as *Cortex magnoliae officinalis* [58], *Withania somnifera* [59], and C. cochinchinense [60], which also exhibit potent antiglycation effects, albeit often at lower concentrations. The variation in effectiveness may stem from differences in active compound concentrations and extraction methods.

The study elucidated the mechanism of action through molecular docking and dynamics simulations, revealing that clove compounds interact with glycation-prone residues, such as lysine and arginine, on BSA. This interaction is consistent with prior research, which identifies lysine residues as highly susceptible to glycation in proteins such as hemoglobin and albumin [61-64]. By binding to these residues, clove compounds may sterically hinder glucose interaction with BSA, preventing AGE formation. Molecular dynamics simulations further supported this by demonstrating stable complexes between clove compounds and BSA under physiological conditions, indicating a targeted and sustained inhibitory effect [65]. The reduction in protein aggregation, as indicated by the decreased aggregation index, underscores the extract's ability to mitigate glycation-induced protein damage, a critical factor in diabetes-related complications. This effect is likely linked to both reduced AGE formation and the preservation of BSA's secondary structure, as evidenced by Congo red and UV-Vis spectroscopy data. Such preservation is vital, as glycation can severely impair protein functionality [62]. The study also compared its findings with similar research, which demonstrated clove bud extract's ability to counteract oxidative stress in human neuroblastoma SH-SY5Y cell lines [65]. This aligns with the current study's emphasis on clove's bioactive compounds and their synergistic effects, suggesting broader therapeutic potential, including for neurodegenerative diseases such as Alzheimer's disease (AD).

Clove bud extract demonstrates significant antiglycation and antioxidant properties in both in vitro and in vivo studies, effectively inhibiting advanced glycation end products (AGEs) and protecting against protein oxidation [66]. While laboratory studies highlight its potential, challenges such as metabolism and bioavailability complicate translating these effects into living organisms. Research indicates that cloves and their active component, eugenol, have beneficial effects in vivo, although these effects are often less pronounced than those observed in vitro [67]. In zebrafish models, clove extract exhibits notable antiglycation, hypolipidemic, and anti-atherosclerotic effects [68]. Moreover, it shows promising anticancer activities in breast carcinoma models by reducing tumor frequency and modifying cancer-related gene expression in vivo, as well as inducing antiproliferative and pro-apoptotic effects in MCF-7 cells in vitro [69].

Our in vitro results demonstrate that clove bud extract can significantly inhibit glycation; however, translating this finding into a food ingredient or therapeutic application requires a realistic approach and further research. Culinary use typically involves small amounts of cloves, such as a teaspoon in a stew or a pinch in spice blends, making it unlikely that dietary intake alone would reach the laboratory concentration used (approximately 600 µg/mL in a closed system). Nonetheless, regular cooking or slight supplementation may increase exposure to active components, especially eugenol, which seems to be fairly bioavailable. Safety has

been confirmed for typical culinary use; however, concentrated supplements should be approached with caution. High doses of eugenol have been linked to liver stress, so careful monitoring is necessary during any high-dose regimen. Moving beyond in vitro results requires thorough in vivo validation and ultimately clinical trials to determine safe and effective dosages and real-world results. Biomarkers such as circulating AGE levels (measured by AGE-specific fluorescence or ELISA) and clinical glycation indicators, such as glycated albumin or HbA1c, which relate to the observed mechanisms, are valid for these studies. Tools like molecular docking provide helpful clues but do not replace biological confirmation; further study of active compounds and potential synergistic effects with other antiglycation agents are essential next steps. Overall, clove bud extract shows promise as a natural candidate for reducing glycation-related damage, with possible uses in both diet and medicine—provided that proper dosing, safety, and efficacy are confirmed through targeted, biomarker-based research.

CONCLUSION

Syzygium aromaticum, commonly known as clove, is recognized for its medicinal properties, but its effects on glycation have only recently been explored. This study examines the impact of clove bud extract on glycation, focusing on BSA. The extract significantly inhibited glycation, reducing browning intensity and aggregation index in glycated BSA while preserving its secondary structure, highlighting its protective role. Molecular docking revealed that clove compounds interact with glycation-prone amino acids such as lysine and arginine, suggesting a targeted antiglycation mechanism. Molecular dynamics simulations confirmed the stability of these interactions under physiological conditions, supporting the potential of clove extract as an effective antiglycation agent in biological systems. These findings position clove bud extract as a promising natural therapeutic for diabetes-related complications and other glycation-linked conditions. The field of antiglycation research has advanced in understanding glycation, a non-enzymatic reaction that produces advanced glycation end products (AGEs), which are associated with chronic diseases. This study highlights achievements, such as identifying natural compounds, including clove bud extract with potent antiglycation properties, and limitations, including a lack of in vivo evidence and variability in the composition of natural extracts. Future research should investigate the effects of clove bud extract on a broader range of proteins, explore its specific antiglycation mechanisms, and examine combination therapies to enhance its efficacy. Addressing these gaps will be crucial for advancing antiglycation strategies in clinical applications. While progress has been made, further exploration is needed to fully realize the therapeutic potential of clove bud extract and other natural inhibitors in the management of glycation-related diseases.

List of abbreviations: AGEs: Advanced Glycation End Products; BSA: Bovine Serum Albumin; CD: Circular Dichroism; DPPH: 2,2-Diphenyl-1-picrylhydrazyl; FTIR: Fourier-Transform Infrared Spectroscopy; MD: Molecular Dynamics; PDB: Protein Data Bank; PE: Potential Energy; RG: Radius Of Gyration; RMSD: Root Mean Square Deviation; RMSF: Root Mean Square Fluctuation; ROS: Reactive Oxygen Species; SASA: Solvent Accessible Surface Area; TE: Total Energy; ThT: Thioflavin T.

Conflicts of Interest: The author declares no conflict of interest.

References

1. Singh RB, Barden A, Mori T, Beilin L. Advanced glycation end-products: a review. Diabetologia. 2001 Feb;44(2):129-46. DOI: https://doi.org/10.1007/s001250051591.
2. Negre-Salvayre A, Salvayre R, Auge N, Pamplona R, Portero-Otin M. Hyperglycemia and glycation in diabetic complications. Antioxidants & redox signaling. 2009 Dec 1;11(12):3071-109. DOI: https://doi.org/10.1089/ars.2009.2484.

3. Ahmed N, Dobler D, Dean M, Thornalley PJ. Peptide mapping identifies hotspot site of modification in human serum albumin by methylglyoxal involved in ligand binding and esterase activity. Journal of Biological Chemistry. 2005 Feb 18;280(7):5724-32. DOI: https://doi.org/10.1074/jbc.M410973200.
4. Yamagishi SI. Role of advanced glycation end products (AGEs) and receptor for AGEs (RAGE) in vascular damage in diabetes. Experimental gerontology. 2011 Apr 1;46(4):217-24. DOI: https://doi.org/10.1016/j.exger.2010.11.007.
5. Adisakwattana S, Sompong W, Meeprom A, Ngamukote S, Yibchok-Anun S. Cinnamic acid and its derivatives inhibit fructose-mediated protein glycation. International journal of molecular sciences. 2012 Feb 8;13(2):1778-89. DOI: https://doi.org/10.3390/ijms13021778.
6. Li XH, Du LL, Cheng XS, Jiang X, Zhang Y, Lv Blet al. Glycation exacerbates the neuronal toxicity of β-amyloid. Cell death & disease. 2013 Jun;4(6):e673-. DOI: https://doi.org/10.1038/cddis.2013.180.
7. Thornalley PJ. Use of aminoguanidine (Pimagedine) to prevent the formation of advanced glycation endproducts. Archives of biochemistry and biophysics. 2003 Nov 1;419(1):31-40. DOI: https://doi.org/10.1016/j.abb.2003.08.013.
8. Safari MR, Azizi O, Heidary SS, Kheiripour N, Ravan AP. Antiglycation and antioxidant activity of four Iranian medical plant extracts. Journal of pharmacopuncture. 2018 Jun 30;21(2):82 DOI: https://doi.org/10.3831/KPI.2018.21.010
9. S Tang SY, Whiteman M, Peng ZF, Jenner A, Yong EL, Halliwell B. Characterization of antioxidant and antiglycation properties and isolation of active ingredients from traditional Chinese medicines. Free Radical Biology and Medicine. 2004 Jun 15;36(12):1575-87. DOI: https://doi.org/10.1016/j.freeradbiomed.2004.03.017.
10. Babu PV, Gokulakrishnan A, Dhandayuthabani R, Ameethkhan D, Kumar CV, Ahamed MI. Protective effect of Withania somnifera (Solanaceae) on collagen glycation and cross-linking. Comparative Biochemistry and Physiology Part B: Biochemistry and Molecular Biology. 2007 Jun 1;147(2):308-13. DOI: https://doi.org/10.1016/j.cbpb.2007.01.011.
11. Xi M, Hai C, Tang H, Chen M, Fang K, Liang X. Antioxidant and antiglycation properties of total saponins extracted from traditional Chinese medicine used to treat diabetes mellitus. Phytotherapy Research: An International Journal Devoted to Pharmacological and Toxicological Evaluation of Natural Product Derivatives. 2008 Feb;22(2):228-37. DOI: https://doi.org/10.1002/ptr.2297.
12. Gutierrez RM, Muñiz-Ramirez A, Campoy AH, Flores JM, Flores SO. Polyphenols of leaves of Apium graveolens inhibit in vitro protein glycation and protect RINm5F cells against methylglyoxal-induced cytotoxicity. Functional Foods in Health and Disease. 2018 Mar 31;8(3):193-211. DOI: https://doi.org/10.31989/ffhd.v8i3.399
13. Shimoda H, Hirano M, Takeda S, Hitoe S. Glucosinolates and isothiocyanates from broccoli seed extract suppress protein glycation and carbonylation. Functional Foods in Health and Disease. 2018 Jan 31;8(1):35-48. DOI: https://doi.org/10.31989/ffhd.v8i1.391
14. Danthu P, Simanjuntak R, Fawbush F, Tsy JL, Razafimamonjison G, Abdillahi MM, et al. The clove tree and its products (clove bud, clove oil, eugenol): prosperous today but what of tomorrow's restrictions?. Fruits. 2020 Sep 24;75(5):224-42 DOI: https://doi.org/10.17660/th2020/75.5.5.
15. Abdul Aziz AH, Rizkiyah DN, Qomariyah L, Irianto I, Che Yunus MA, Putra NR. Unlocking the full potential of clove (*Syzygium aromaticum*) spice: an overview of extraction techniques, bioactivity, and future opportunities in the food and beverage industry. Processes. 2023 Aug 15;11(8):2453. DOI: https://doi.org/10.3390/pr11082453
16. Perera HK, Wijetunge DC. Strong protein glycation inhibitory potential of clove and coriander. British J Pharmaceutical Res. 2015 Jun 3;6(5):306-12. DOI: https://doi.org/10.9734/BJPR/2015/16190.
17. Perera HK, Wijetunge DC. Strong protein glycation inhibitory potential of clove and coriander. British J Pharmaceutical Res. 2015 Jun 3;6(5):306-12. DOI: https://doi.org/10.9734/BJPR/2015/16190.
18. Cheikhyoussef A, Cheikhyoussef N, Rahman A, Hussein AA. Clove (*Syzygium aromaticum*) phenolics: Extraction, compositions, and biological activities. InClove (*Syzygium aromaticum*) 2022 Jan 1 (pp. 215-233). Academic Press. DOI: https://doi.org/10.1016/B978-0-323-85177-0.00036-7.
19. Indiarto R, Herwanto JA, Filianty F, Lembong E, Subroto E, Muhammad DR. Total phenolic and flavonoid content, antioxidant activity and characteristics of a chocolate beverage incorporated with encapsulated clove bud extract. CyTA-Journal of Food. 2024 Dec 31;22(1):2329144. DOI: https://doi.org/10.1080/19476337.2024.2329144.
20. Mansour HM, Zeitoun AA, Abd-Rabou HS, El Enshasy HA, Dailin DJ, Zeitoun MA. Antioxidant and anti-diabetic properties of olive (Olea europaea) leaf extracts: In vitro and in vivo evaluation. Antioxidants. 2023 Jun 14;12(6):1275. DOI: https://doi.org/10.3390/antiox12061275.

21. Agu MC, Omebere TF. Evaluation of Antibacterial Activities of Clove Bud Oil and Extract on Bacterial Isolates from Dental Caries. Glob Acad J Dent Oral Health. 2024;6. DOI: https://doi.org/10.36348/gajdoh.2024.v06i03.001.
22. Lone ZA, Jain NK. Phytochemical analysis of clove (*Syzygium aromaticum*) dried flower buds extract and its therapeutic importance. Journal of Drug Delivery and Therapeutics. 2022 Jul 2;12(4-S):87-92. DOI: https://doi.org/10.22270/jddt.v12i4-S.5628.
23. Brownlee M, Vlassara H, Kooney A, Ulrich P, Cerami A. Aminoguanidine prevents diabetes-induced arterial wall protein cross-linking. Science. 1986 Jun 27;232(4758):1629-32. DOI: https://doi.org/10.1126/science.3487117.
24. Anwar S, Almatroudi A, Allemailem KS, Jacob Joseph R, Khan AA, Rahmani AH. Protective effects of ginger extract against glycation and oxidative stress-induced health complications: An in vitro study. Processes. 2020 Apr 16;8(4):468. DOI: https://doi.org/10.3390/pr8040468.
25. Schrödel A, de Marco A. Characterization of the aggregates formed during recombinant protein expression in bacteria. BMc Biochemistry. 2005 May 31;6(1):10. DOI: https://doi.org/10.1186/1471-2091-6-10.
26. Klunk WE, Jacob RF, Mason RP. Quantifying amyloid by congo red spectral shift assay. InMethods in enzymology 1999 Jan 1 (Vol. 309, pp. 285-305). Academic Press. DOI: https://doi.org/10.1016/S0076-6879(99)09021-7.
27. Alsahli M, Anwar S, Alzahrani FM, Almatroudi A, Alfheeaid H, Khan AA. Health promoting effect of Phyllanthus emblica and Azadiractha indica against advanced glycation end products formation. Applied Sciences. 2021 Sep 23;11(19):8819. DOI: https://doi.org/10.3390/app11198819
28. Anwar S, Khan MA, Sadaf A, Younus H. A structural study on the protection of glycation of superoxide dismutase by thymoquinone. International journal of biological macromolecules. 2014 Aug 1;69:476-81. DOI: https://doi.org/10.1016/j.ijbiomac.2014.06.003.
29. S Panigrahi SK, Mishra AK. Inner filter effect in fluorescence spectroscopy: As a problem and as a solution. Journal of Photochemistry and Photobiology C: Photochemistry Reviews. 2019 Dec 1;41:100318. DOI: https://doi.org/10.1016/j.jphotochemrev.2019.100318.
30. Razafimamonjison G, Jahiel M, Duclos T, Ramanoelina P, Fawbush F, Danthu P. Bud, leaf and stem essential oil composition of *Syzygium aromaticum* from Madagascar, Indonesia and Zanzibar. International Journal of Basic and Applied Sciences. 2014 Jul 1;3(3):224. DOI: https://doi.org/10.14419/ijbas.v3i3.2473.
31. Rosarior VL, Lim PS, Wong WK, Yue CS, Yam HC, Tan SA. Antioxidant-rich clove extract, a strong antimicrobial agent against urinary tract infections-causing bacteria in vitro. Tropical Life Sciences Research. 2021 Jun 29;32(2):45. DOI: https://doi.org/10.21315/tlsr2021.32.2.4.
32. Trott O, Olson AJ. AutoDock Vina: improving the speed and accuracy of docking with a new scoring function, efficient optimization, and multithreading. Journal of computational chemistry. 2010 Jan 30;31(2):455-61. DOI: https://doi.org/10.1002/jcc.21334.
33. Pandya P, Agarwal LK, Gupta N, Pal S. Molecular recognition pattern of cytotoxic alkaloid vinblastine with multiple targets. Journal of Molecular Graphics and Modelling. 2014 Nov 1;54:1-9. DOI: https://doi.org/10.1016/j.jmgm.2014.09.001.
34. Morris GM, Goodsell DS, Halliday RS, Huey R, Hart WE, Belew RK et al. Automated docking using a Lamarckian genetic algorithm and an empirical binding free energy function. Journal of computational chemistry. 1998 Nov 15;19(14):1639-62. DOI:https://doi.org/10.1002/(SICI)1096-987X(19981115)19:14<1639::AID-JCC10>3.0.CO;2-B.
35. Wang J, Wolf RM, Caldwell JW, Kollman PA, Case DA. Development and testing of a general amber force field. Journal of computational chemistry. 2004 Jul 15;25(9):1157-74. DOI: https://doi.org/10.1002/jcc.20035.
36. Berendsen HJ, van der Spoel D, van Drunen R. GROMACS: A message-passing parallel molecular dynamics implementation. Computer physics communications. 1995 Sep 2;91(1-3):43-56. DOI: https://doi.org/10.1016/0010-4655(95)00042-E.
37. Hornak V, Abel R, Okur A, Strockbine B, Roitberg A, Simmerling C. Comparison of multiple Amber force fields and development of improved protein backbone parameters. Proteins: Structure, Function, and Bioinformatics. 2006 Nov 15;65(3):712-25. DOI: https://doi.org/10.1002/prot.21123.
38. Bussi G, Donadio D, Parrinello M. Canonical sampling through velocity rescaling. The Journal of chemical physics. 2007 Jan 7;126(1). DOI: https://doi.org/10.1063/1.2408420.
39. Parrinello M, Rahman A. Polymorphic transitions in single crystals: A new molecular dynamics method. Journal of Applied physics. 1981 Dec 1;52(12):7182-90. DOI: https://doi.org/10.1063/1.328693.

40. Kumari R, Kumar R, Open Source Drug Discovery Consortium, Lynn A. g_mmpbsa A GROMACS tool for high-throughput MM-PBSA calculations. Journal of chemical information and modeling. 2014 Jul 28;54(7):1951-62. DOI: https://doi.org/10.1021/ci500020m.
41. Qiao J, Wang X, Liu L, Zhang H. Nonenzymatic browning and protein aggregation in royal jelly during room-temperature storage. Journal of Agricultural and Food Chemistry. 2018 Feb 28;66(8):1881-8. DOI: https://doi.org/10.1021/acs.jafc.7b04955.
42. Liu X, Liu J, Zhang W, Pearce R, Chen M, Zhang T, Liu B. Effect of the degree of glycation on the stability and aggregation of bovine serum albumin. Food Hydrocolloids. 2020 Sep 1; 106:105892. DOI: https://doi.org/10.1016/j.foodhyd.2020.105892.
43. Rubab U, Kumar D, Farah MA, Al-Anazi KM, Ali MA, Ali A. Inhibitory roles of Nigella sativa seed extracts on in vitro glycation and aggregation. Pharmacognosy Magazine. 2021;17(06). DOI: https://doi.org/10.4103/pm.pm_604_20.
44. Sherwani S, Rajendrasozhan S, Khan MW, Saleem M, Khan M, Khan S, Raafat M, Othman Alqahtani F. Pharmacological profile of Nigella sativa seeds in combating COVID-19 through in-vitro and molecular docking studies. Processes. 2022 Jul 11;10(7):1346. DOI: https://doi.org/10.3390/pr10071346.
45. Ahmad J, Alam K. Impact of in vitro non-enzymatic glycation on biophysical and biochemical regimes of human serum albumin: relevance in diabetes associated complications. RSC Advances. 2015;5(78):63605-14. DOI: https://doi.org/10.1039/C5RA07232H.
46. Riaz S, Siddiqui S, Abul Qais F, Mateen S, Moin S. Inhibitory effect of baicalein against glycation in HSA: An in vitro approach. Journal of Biomolecular Structure and Dynamics. 2024 Jan 22;42(2):935-47. DOI: https://doi.org/10.1080/07391102.2023.2201856.
47. Qais FA, Sarwar T, Ahmad I, Khan RA, Shahzad SA, Husain FM. Glyburide inhibits non-enzymatic glycation of HSA: An approach for the management of AGEs associated diabetic complications. International Journal of Biological Macromolecules. 2021 Feb 1; 169:143-52. DOI: https://doi.org/10.1016/j.ijbiomac.2020.12.096.
48. Mishra A, Abul Qais F, Pathak Y, Camps I, Tripathi V. Triamcinolone as a Potential Inhibitor of SARS-CoV-2 Main Protease and Cytokine Storm: An In silico Study. Letters in Drug Design & Discovery. 2023 Sep 1;20(9):1230-42. DOI: https://doi.org/10.2174/1570180819666220401142351.
49. Fouedjou RT, Chtita S, Bakhouch M, Belaidi S, Ouassaf M, Djoumbissie LA, et al. Cameroonian medicinal plants as potential candidates of SARS-CoV-2 inhibitors. Journal of Biomolecular Structure and Dynamics. 2022 Nov 26;40(19):8615-29. DOI: https://doi.org/10.1080/07391102.2021.1914170.
50. Siddiqui S, Ameen F, Kausar T, Nayeem SM, Rehman SU, Tabish M. Biophysical insight into the binding mechanism of doxofylline to bovine serum albumin: An in vitro and in silico approach. Spectrochimica Acta Part A: Molecular and Biomolecular Spectroscopy. 2021 Mar 15; 249:119296. DOI: https://doi.org/10.1016/j.saa.2020.119296.
51. Chtita S, Fouedjou RT, Belaidi S, Djoumbissie LA, Ouassaf M, Qais FA. In silico investigation of phytoconstituents from Cameroonian medicinal plants towards COVID-19 treatment. Structural Chemistry. 2022 Oct;33(5):1799-813. DOI: https://doi.org/10.1007/s11224-022-01939-7.
52. Ansari NA, Moinuddin, Ali R. Glycated lysine residues: a marker for non-enzymatic protein glycation in age-related diseases. Disease markers. 2011;30(6):317-24. DOI: https://doi.org/10.3233/DMA-2011-0791.
53. Martirosyan D. Functional Food Science and Bioactive Compounds. Bioactive Compounds in Health and Disease-Online ISSN: 2574-0334; Print ISSN: 2769-2426. 2025 Jul 1;8(6):218-29. DOI: https://doi.org/10.31989/bchd.v8i6.1667
54. Xie B, Chen P, Hong Y, Xu C, Zhang W. Effects of a dietary compound tablet on glucose metabolism in a hyperglycemic mouse model. Dietary Supplements and Nutraceuticals. 2025 Jun 6;4(06):1-1. DOI: https://doi.org/10.31989/dsn.v4i6.1621
55. David Z, Bashir A, Amoka A, Idris E, Anoze A, Moyosore A, et al. Antioxidant and hepatoprotective activities of methanol extract of Moringa oleifera leaves in carbon tetrachloride-induced hepatotoxicity in rats: Implications for functional food development. Agriculture and Food Bioactive Compounds-Online ISSN: 3068-8051. 2025 Jul 25;2(7):157-70. DOI: https://doi.org/10.31989/AFBC.v2i7.1722
56. Almatroodi SA, Rahmani AH. Unlocking the pharmacological potential of myricetin against various pathogenesis. International Journal of Molecular Sciences. 2025 Apr 28;26(9):4188. DOI: https://doi.org/10.3390/ijms26094188
57. Rahmani AH, Alharbi HO, Khan AA, Babiker AY, Alam Rizvi MM. Therapeutic potential of resveratrol, a polyphenol in the prevention of liver injury induced by diethylnitrosamine

(DEN) through the regulation of inflammation and oxidative stress. Functional Foods in Health & Disease. 2024 Dec 1;14(12). DOI: https://doi.org/10.31989/ffhd.v14i12.1502

58. Tang SY, Whiteman M, Peng ZF, Jenner A, Yong EL, Halliwell B. Characterization of antioxidant and antiglycation properties and isolation of active ingredients from traditional Chinese medicines. Free Radical Biology and Medicine. 2004 Jun 15;36(12):1575-87. DOI: https://doi.org/10.1016/j.freeradbiomed.2004.03.017.
59. Babu PV, Gokulakrishnan A, Dhandayuthabani R, Ameethkhan D, Kumar CV, Ahamed MI. Protective effect of Withania somnifera (Solanaceae) on collagen glycation and cross-linking. Comparative Biochemistry and Physiology Part B: Biochemistry and Molecular Biology. 2007 Jun 1;147(2):308-13. DOI: https://doi.org/10.1016/j.cbpb.2007.01.011.
60. A Parveen A, Sultana R, Lee SM, Kim TH, Kim SY. Phytochemicals against anti-diabetic complications: targeting the advanced glycation end product signaling pathway. Archives of Pharmacal Research. 2021 Apr;44(4):378-401. DOI: https://doi.org/10.1007/s12272-021-01323-9.
61. Anwar S, Khan MA, Sadaf A, Younus H. A structural study on the protection of glycation of superoxide dismutase by thymoquinone. International journal of biological macromolecules. 2014 Aug 1; 69:476-81. DOI: https://doi.org/10.1016/j.ijbiomac.2014.06.003.
62. Ahmed N, Dobler D, Dean M, Thornalley PJ. Peptide mapping identifies hotspot site of modification in human serum albumin by methylglyoxal involved in ligand binding and esterase activity. Journal of Biological Chemistry. 2005 Feb 18;280(7):5724-32. DOI: https://doi.org/10.1074/jbc.M410973200.
63. Ahmad J, Alam K. Impact of in vitro non-enzymatic glycation on biophysical and biochemical regimes of human serum albumin: relevance in diabetes associated complications. RSC Advances. 2015;5(78):63605-14. DOI: https://doi.org/10.1039/C5RA07232H.
64. Riaz M, Khalid R, Afzal M, Anjum F, Fatima H, Zia S, Rasool G, Egbuna C, Mtewa AG, Uche CZ, Aslam MA. Phytobioactive compounds as therapeutic agents for human diseases: a review. Food Sci Nutr. 2023, 11 (6): 2500–2529. DOI: https://doi.org/10.1002/fsn3.3308.
65. Sharma H, Kim DY, Shim KH, Sharma N, An SS. Multi-targeting neuroprotective effects of *Syzygium aromaticum* bud extracts and their key phytocompounds against neurodegenerative diseases. International Journal of Molecular Sciences. 2023 May 2;24(9):8148. DOI: https://doi.org/10.3390/ijms24098148.
66. Suantawee T, Wesarachanon K, Anantsuphasak K, Daenphetploy T, Thien-Ngern S, Thilavech T, et al. Protein glycation inhibitory activity and antioxidant capacity of clove extract. Journal of food science and technology. 2015 Jun;52(6):3843-50. DOI: https://doi.org/10.1007/s13197-014-1452-1.
67. Yu B, Li C, Gu L, Zhang L, Wang Q, Zhang Yet al. Eugenol protects against Aspergillus fumigatus keratitis by inhibiting inflammatory response and reducing fungal load. European Journal of Pharmacology. 2022 Jun 5; 924:174955. DOI: https://doi.org/10.1016/j.ejphar.2022.174955.
68. Jin S, Cho KH. Water extracts of cinnamon and clove exhibits potent inhibition of protein glycation and anti-atherosclerotic activity in vitro and in vivo hypolipidemic activity in zebrafish. Food and Chemical Toxicology. 2011 Jul 1;49(7):1521-9. DOI: https://doi.org/10.1016/j.fct.2011.03.043.
69. Kubatka P, Uramova S, Kello M, Kajo K, Kruzliak P, Mojzis J, et al. Antineoplastic effects of clove buds (*Syzygium aromaticum* L.) in the model of breast carcinoma. Journal of Cellular and Molecular Medicine. 2017 Nov;21(11):2837-51. DOI: https://doi.org/10.1111/jcmm.13197.